[P3]

V. Viikari, J. Mallat, J. Ala-Laurinaho, J. Häkli, and A. Räisänen, “A frequency shift technique for pattern correction in hologram-based CATRs,” *IEEE Transactions on Antennas and Propagation*, vol. 54, no. 10, pp 2963 – 2968, Oct. 2006.

A Frequency Shift Technique for Pattern Correction in Hologram-Based CATRs

Ville Viikari, *Student Member, IEEE*, Juha Mallat, Juha Ala-Laurinaho, Janne Häkli, *Member, IEEE*, and Antti V. Räisänen, *Fellow, IEEE*

***Abstract*—The measurement accuracy of a compact antenna test range (CATR) is limited by the level of spurious signals. At millimeter and submillimeter wavelengths the spurious signals are caused by range reflections and deformations of the range collimating element. Several antenna pattern and range evaluation techniques that can be used to mitigate the effects of these nonidealities have been published. At submillimeter wavelengths these techniques are typically time consuming or they are not able to correct the antenna pattern close to the main beam. The frequency shift technique does not have these limitations in a hologram based CATR. In this paper, the applicability of the frequency shift technique is analytically studied for a hologram based CATR. The technique is verified by measurements. The accuracy provided by the frequency shift technique is compared to that of the antenna pattern comparison (APC) technique.**

***Index Terms*—Antenna measurements, compact range, error compensation, submillimeter wave measurements.**

I. Introduction

THE measurement accuracy of a compact antenna test range (CATR) is limited by the level of the spurious signals. The level of the spurious signal should be much lower than the side lobe level of the antenna under test (AUT). Spurious signals are caused by the unwanted reflections in the range. Also inaccuracies and deformations of the range reflector may cause distortions at millimeter and submillimeter wavelengths, because the tight surface accuracy requirements of about one hundredth of the wavelength can not be fully satisfied. The surface accuracy requirement can be reduced by using a transmission-type hologram as a collimating element [1].

A hologram is a diffractive grating, which transforms a spherical wave front into a plane wave. The computer generated grating pattern is etched on a copper-plated mylar film. The hologram based CATR has shown its potential for measuring large submillimeter wave antennas [2]–[4]. The main challenge with large holograms is the current manufacturing technology. Large ($>$1 m) holograms have to be manufactured from several pieces. The seams and the misalignment between pieces decrease the quiet-zone quality.

Manuscript received February 20, 2006; revised May 10, 2006. This work was supported in part by the Center of Excellence Program of the Academy of Finland and Tekes, by the Foundation of the Finnish Society of Electronic Engineers, by the Foundation for Commercial and Technical Sciences, by the Foundation of Technology, and by the Graduate School of Electrical and Communications Engineering.

The authors are with the MilliLab, Radio Laboratory/SMARAD, Helsinki University of Technology, Espoo FI-02015 TKK, Finland (e-mail: ville.viikari@tkk.fi).

Digital Object Identifier 10.1109/TAP.2006.882175

Several antenna pattern correction and range evaluation techniques have been developed to mitigate the effects of the nonidealities. Suitable correction techniques at submillimeter wavelengths are time gating [5], antenna pattern comparison (APC) [6], feed scanning based APC [7], and frequency shifting [8], [9]. The limitation with the time gating technique is that it is not able to correct spurious signals caused by the collimating element. This limits the pattern correction only to distant side lobes when electrically large antennas are measured. APC and feed scanning APC are effective also close to the main beam, but the measurement time increases significantly when correcting the antenna pattern even only in one dimension. Pattern correction in two dimensions is extremely time-consuming, as the AUT has to be moved both vertically and horizontally.

A frequency shift method is very practical pattern correction and range evaluation technique at submillimeter wavelengths. The method is easy to implement, and the measurement time does not increase significantly, because measurements at different frequencies can be performed rapidly with network analyzers. This enables pattern correction even in two dimensions. The frequency shift method was introduced already in the early era of anechoic chambers [8]. At that time the method was used at low radio frequencies, and it was not seen attractive due to its large relative bandwidth requirements. However, at millimeter and submillimeter wavelengths the required bandwidth is relatively small. For example, the required bandwidth is approximately $\pm 1\%$ in the test case introduced later.

In reflector- or lens-based CATRs the frequency shift technique has the same limitation as the time gating. The correction is limited only to distant side lobes at submillimeter wavelengths. In the hologram-based CATRs, the method is also able to compensate some amount of distortions caused by the hologram. In this paper, the applicability of the frequency shift method in a hologram-based CATR is studied.

In Section II, we introduce the principle of the method and discuss its feasibility. Section III introduces the verification procedure and measurement setup with the method. The results are presented in Section IV and conclusions in Section V.

II. Frequency Shift-Based APC Technique

Let us consider a hologram-based CATR, in which the quiet-zone plane wave is disturbed by a spurious signal (Fig. 1). In the frequency shift technique, the antenna pattern is measured several times at slightly different frequencies. At each frequency, the spurious signal sums in different phase to the direct signal because the electrical path lengths of the signals change differently with the frequency. Finally, the effect of the spurious signal can be cancelled out by averaging the results measured

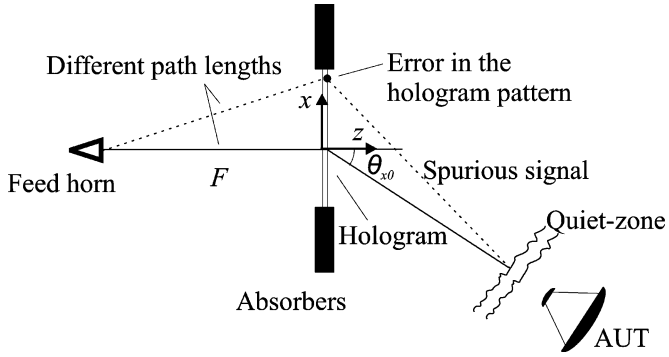

Fig. 1. Hologram-based CATR with a disturbance in the hologram pattern.

at different frequencies. As the hologram is a planar structure, the signal path length to the edge of the hologram is longer than that to the center of the hologram (Fig. 1). This enables partial correction of the non-ideal operation of the hologram, such as edge diffraction disturbances.

A. Maximum Bandwidth of the Hologram

On the contrary to a reflector or a lens, a hologram is a dispersive structure, and its bandwidth requirements have to be taken into account. The transmitted field of the hologram $E_{\rm tr}$ can be calculated from the incident field $E_{\rm in}$ with a complex transmittance function $T(x,y)$ as [1]

$$E_{\rm tr}(x,y) = T(x,y)E_{\rm in}(x,y). \tag{1}$$

In CATRs, the hologram modulates the phase and the amplitude of the incident field so that the transmitted spherical wave front is transformed into a plane wave with edge taper. When the frequency and, thus, also the wavelength is changed, the phase of the incident field is changed. According to (1), a phase change of the incident field introduces a phase change to the transmitted field. The geometrically derived phase change of the incident field and thus also the transmitted field at the wavelength of λ is

$$\Delta\psi_{\rm tr}(x,\lambda) = 2\pi\sqrt{F^2+x^2}\left(\frac{1}{\lambda_0}-\frac{1}{\lambda}\right) \tag{2}$$

where F is the focal length of the hologram, x is the horizontal coordinate on the hologram surface (y-coordinate is assumed to be zero for simplicity) and λ_0 is the wavelength at the center frequency. The incident phase affects directly the transmitted phase and it is approximately the phase also in the quiet-zone, because the field conserves its shape well during the propagation. As a function of x, (2) introduces a constant phase term and a nonlinear phase term. A constant phase shift is harmless because the phase of the measured pattern is anyway normalized. The nonlinear phase term has to be taken into account, because it degrades the quiet-zone quality and decreases the measurement accuracy. The nonlinear part of (2) is (the phase is normalized to zero in the center of the hologram)

$$\Delta\psi_{\rm tr,N}(x,\lambda) = 2\pi(\sqrt{F^2+x^2}-F)\left(\frac{1}{\lambda_0}-\frac{1}{\lambda}\right). \tag{3}$$

The shape of the phase curvature in (3) is similar to the phase curvature in the far-field ranges. Therefore, using the typical far-field criteria, the phase curvature should not exceed 22.5° ($\pi/8$ in radians) in the aperture of the AUT when the frequency is shifted. A more stringent far-field criterion should be used when performing extremely accurate measurements [10]. Despite that we are aiming at accurate measurements, we can accept a looser criterion, because the method is able to correct some amount of unwanted effects caused by the phase curvature (due to frequency shift).

The largest phase deviations occur at the edges of the aperture of the AUT and, thus, the largest and the smallest allowed wavelengths can be solved by substituting $\Delta\psi_{\rm tr,N}(x = D_{\rm AUT}/2,\lambda) = \pi/8$ into (3)

$$\frac{1}{\lambda} = \frac{1}{\lambda_0} \pm \frac{1}{16\left(\sqrt{F^2+(D_{\rm AUT}/2)^2}-F\right)} \tag{4}$$

where $D_{\rm AUT}$ is the aperture diameter of the AUT. The relative bandwidth of the hologram can be solved from (4) as

$$\frac{\Delta f}{f_0} = \pm\frac{\lambda_0}{16\left(\sqrt{F^2+(D_{\rm AUT}/2)^2}-F\right)} \tag{5}$$

where Δf is the absolute deviation from the center frequency f_0. For example, when the focal length of the hologram is 1.8 m and the AUT diameter is 76.2 mm, the relative bandwidth at 310 GHz is ±15.0%.

In addition to the phase curvature, there are some minor effects to the quiet-zone field due to a frequency shift. When the frequency is changed, the radiation pattern of the range feed antenna may slightly change. Usually, illumination remains practically unchanged, because a broadband horn antenna is employed as a range feed. Another effect is that the direction of the plane wave is slightly steered. Typically, holograms are designed to produce a plane wave propagating to an offset angle $\theta_{\rm x0}$ from the normal of the hologram surface, in order to prevent unwanted diffraction modes from disturbing the quiet-zone field. The spatial frequency of the transmitted field at the center frequency is

$$\nu = \frac{\sin\theta_{\rm x0}}{\lambda_0}. \tag{6}$$

The spatial frequency depends mainly on the hologram grating constant and does not change with the frequency in the center of the hologram. The steered direction θ of the plane wave can be solved from (6) by assuming that the spatial frequency remains unchanged

$$\theta = \arcsin\left(\frac{\lambda}{\lambda_0}\sin\theta_{x0}\right). \tag{7}$$

The whole aperture of the AUT should remain in the quiet-zone when the frequency is shifted. Normally, the steering is so small, that it does not need to be taken into account. For example, if the original direction of the plane wave is 33° at 310 GHz, the

steered direction at 313.5 GHz is 32.6°. Another effect is that the angle between the mechanical axis and the electrical axis in the test range is changed. Therefore, the antenna pointing angle is measured at the center frequency, and the antenna patterns measured at other frequencies are shifted in angular domain so, that the main beam direction is 0°.

B. Maximum Bandwidth of the AUT

The antenna pattern of the AUT should remain unchanged in the whole frequency range in which the averaging is performed. Hologram CATRs are generally used to measure reflector or lens antennas. These antenna structures are very broadband. Let us assume that there are no multiple reflections inside the antenna structure and that the characteristics of the antenna feed do not change with the frequency. In such a case, the electrical size of the antenna aperture is changed with the frequency. As a consequence, the antenna pattern is scaled in the wave number domain. The scaled x-component of the wave vector at the wavelength of λ can be calculated from

$$k_{\mathrm{x}} = \frac{\lambda}{\lambda_0} k_{\mathrm{x0}} \tag{8}$$

where k_{x0} is the x-component of the wave vector at the center frequency. Assume, that α is a horizontal angle of the antenna pattern at the wavelength of λ (angle in the xz-plane) and that α is defined to be zero in the direction of the main beam of the AUT. Then, the x-component of the wave vector can be written as

$$k_{\mathrm{x}} = k \sin \alpha \tag{9}$$

where k is the wave number. At small angles, (8) can be approximated as

$$\alpha = \frac{\lambda}{\lambda_0} \alpha_0 \tag{10}$$

where α is the scaled angle in the antenna pattern and α_0 is the corresponding angle at the center frequency. On the other hand, the width of a side lobe in radians is approximately $\lambda / D_{\mathrm{AUT}}$. The maximum shift in the antenna pattern should be much smaller than the width of a side lobe

$$\frac{\Delta\lambda}{\lambda_0} \alpha_{\mathrm{MAX}} \ll \frac{\lambda_0}{D_{\mathrm{AUT}}} \tag{11}$$

where $\Delta\lambda$ is the change of the wavelength and α_{MAX} is the maximum angle of the antenna pattern, where the correction is performed. For example, the angular shift at 10° is 15% of the width of the side lobe, if the original frequency of 310 GHz is shifted 3.5 GHz and the antenna diameter is 76.2 mm. If the maximum shift of the antenna pattern is large compared to the width of the side lobe, the measured antenna patterns can be scaled in angular domain before averaging.

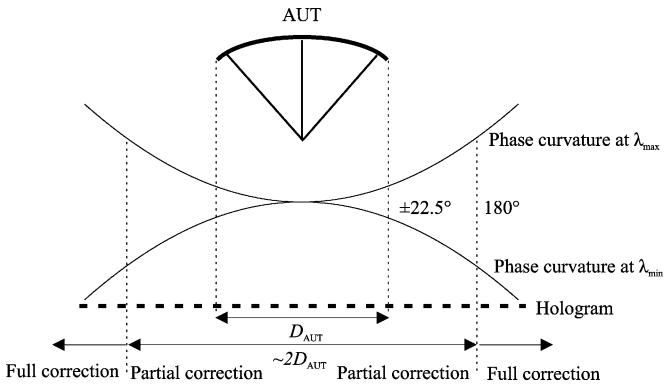

Fig. 2. Correction efficiency of the frequency shift method. For simplicity, the figure is not in scale and the 33° offset angle of the hologram is omitted.

C. Correction Efficiency

The correction efficiency of the frequency shift method depends on the amount of the frequency shift, i.e. the used bandwidth. The frequency shift should be selected so, that the relative change of the phase between direct and spurious signal is 180°. The needed frequency shift is

$$\Delta f = \frac{c}{2\Delta l} \tag{12}$$

where c is the speed of light and Δl is the path length difference between the direct and spurious signal. The bandwidth is limited by the AUT or the hologram. At submillimeter wavelengths, it is likely that the bandwidth is limited by the hologram because the hologram is a dispersive element whereas submillimeter antennas tend to be broadband. In such cases, the minimum required path length difference of the direct and spurious signal can be calculated by substituting (12) into (5)

$$\Delta l = 4 \left(\sqrt{F^2 + (D_{\mathrm{AUT}}/2)^2} - F \right). \tag{13}$$

According to (13), the correction efficiency depends only on the focal length of the hologram and the diameter of the AUT. It can be geometrically calculated using (13), how far from the hologram center the spurious signal has to originate, in order for the method to be able to compensate its effect. The required distance is approximately D_{AUT} with a slight dependence on the geometry, (Fig. 2).

The quiet-zone diameter is generally 50%–60% of the hologram diameter and the AUT is at least slightly smaller than the quiet-zone. Thereby any distortions originating close to the hologram edges can be fully corrected and distortions originating closer to hologram center can be partially corrected.

III. Test Procedure and Measurement Setup

The frequency shift method is tested by measuring antenna patterns of a physical and a virtual test antenna. In both cases, the results with the frequency shift method are compared to the results obtained with the APC technique. The tests with a physical antenna are needed to verify the proposed method in a real environment. However, the antenna pattern of the physical test

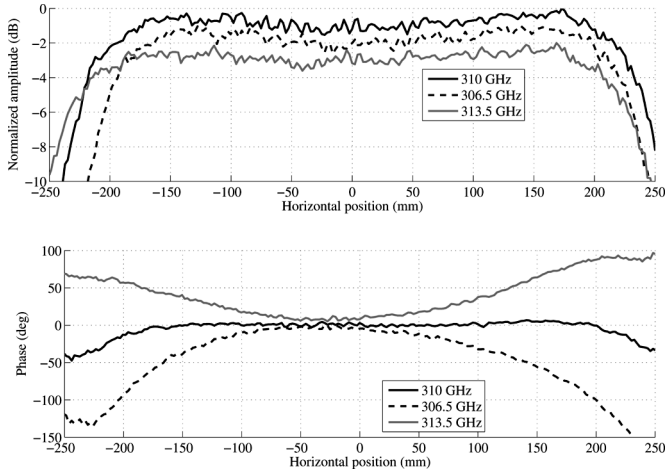

Fig. 3. Measured quiet-zone field cuts at the center frequency and at both extreme frequencies. The lines are shifted for clarity.

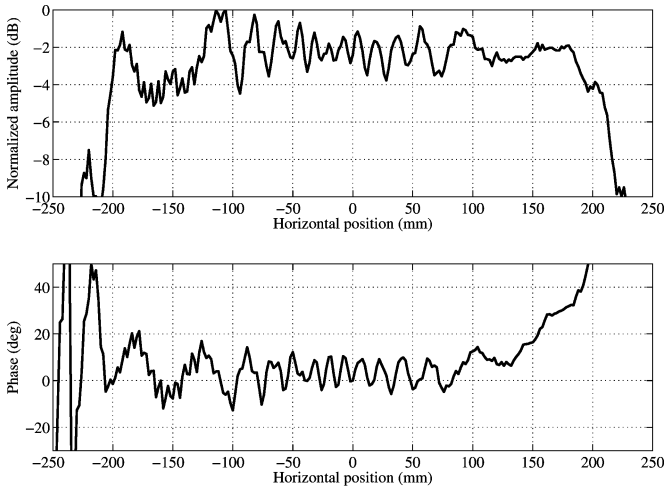

Fig. 4. Horizontal cut of the distorted quiet-zone field used with the virtual antenna.

antenna is not exactly known, and the correction accuracy of the method can not be determined. Accuracies provided by the APC and the frequency shift methods are easy to compare from the results with the virtual antenna, because the antenna pattern of the virtual antenna can be analytically calculated. The test with the virtual antenna is based partly on the measurements and partly on the simulations. The two-dimensional (2-D) quiet-zone field is first probed at different frequencies. The antenna pattern measurements are then simulated at each frequency by calculating the measured patterns with the equation

$$P_{\mathrm{meas}}(k_x, k_y) = \iint E_{\mathrm{qz}} \cdot E_{\mathrm{aper}} \cdot e^{-j(k_k x + k_y y)} dx \cdot dy \quad (14)$$

where E_{qz} is the measured electrical field of the quiet-zone at the main polarization, E_{aper} is the simulated aperture field of the virtual antenna at the main polarization, k_x and k_y are x- and y-components of the wave vector.

The tests are carried out in a hologram-based CATR. The focal length of the hologram is 1.8 m and the hologram diameter is 600 mm. The hologram is designed to operate at 310 GHz. The antenna patterns of the both antennas are measured at frequencies from 306.5 to 313.5 GHz with a frequency interval of 500 MHz. The corrected patterns are obtained by averaging the measured patterns. The main peaks of the patterns are shifted to 0° in angular domain and the phase is normalized to 0° in the center of the main beam before averaging. For demonstration, the hologram operation is intentionally distorted by attaching plastic and metal strips on the hologram surface. The strips are seen approximately in the angles of $\pm 5°$ from the AUT. In the APC method, the antenna patterns of both antennas are measured 15 times at 310 GHz. The AUT is moved 5 mm transversally between every measurement. The averaging with the APC is performed in a similar way as the averaging with the frequency shift method.

Both, the virtual and the physical test antennas are similar. The antennas are based on a single 90° offset fed reflector. The reflector diameter is 76.2 mm and its effective focal length is 127 mm. The virtual antenna has a Gaussian illumination with -12 dB amplitude taper. The aperture fields of the virtual antenna at different frequencies are simulated with GRASP8W-software.[1] In virtual antenna measurements, a planar scanner is employed in the quiet-zone field probing and a corrugated horn is used as a probe antenna.

A commercially available mirror is used as a reflector of the test antenna. The reflector is fed with a corrugated horn. The beam of the horn is nearly Gaussian with -12 dB amplitude taper on the edges of the reflector. Supporting structures of the test antenna are covered with absorbers in order to get good correspondence between the measurements and the simulations.

IV. Experimental Results

A. Quiet-Zone Fields

Fig. 3 depicts the quiet-zone field cuts at the center frequency and at both extreme frequencies.

When the frequency is changed, the amplitude of the quiet-zone field remains almost unchanged while the phase of the quiet-zone field becomes curved as in Fig. 2. The general criteria for the quiet-zone are fulfilled at every frequency in the aperture of the AUT. As mentioned previously, the quiet-zone field was intentionally distorted during the antenna measurements. The distorted quiet-zones used with the virtual antenna and the test antenna slightly differ from each other. The both distorted quiet-zones have approximately a 2 dB ripple in the amplitude and a 15° ripple in the phase, peak-to-peak in the aperture of the AUT. Figs. 4 and 5 presents horizontal cuts of the distorted quiet-zones used with the virtual antenna and test antenna, respectively.

B. Antenna Patterns of the Virtual Antenna

The antenna patterns of the virtual antenna are depicted in Fig. 6. The measured antenna pattern has spurious side lobes around 5° and $-5°$. The spurious side lobe level is 18 dB above the true side lobe level. After the correction with the frequency shift method, the maximum deviation from the true pattern is

[1]http://www.ticra.com.

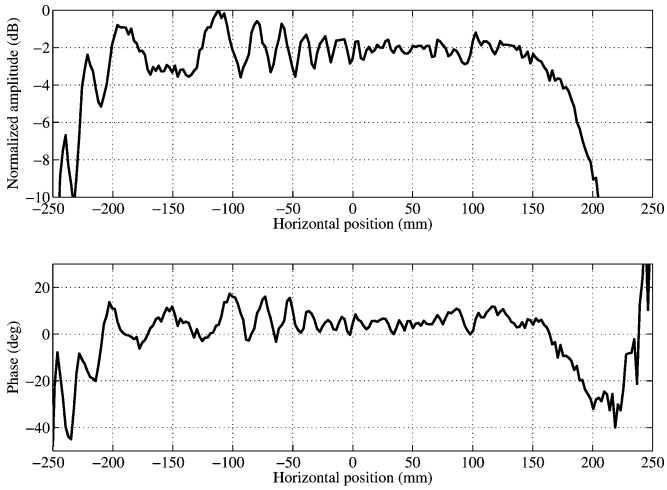

Fig. 5. Horizontal cut of the distorted quiet-zone field used with the test antenna.

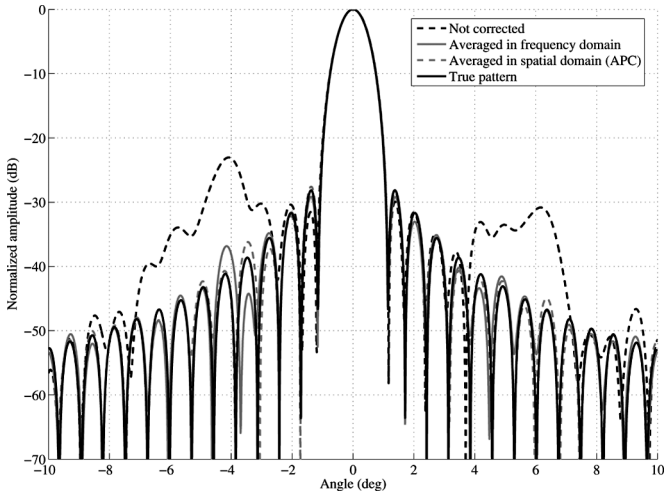

Fig. 6. Antenna patterns of the virtual antenna. The solid black line is the true pattern, the dashed black line is the noncorrected pattern, the solid gray line is the pattern obtained with frequency shift method and the dashed gray line is the pattern obtained with the APC technique.

5 dB at a −40-dB level. The accuracy provided by the APC technique is equally good.

C. Antenna Patterns of the Test Antenna

The antenna patterns of the test antenna are shown in Fig. 7. The measured antenna pattern is corrupted from -8° to -2° and from 4° to 8°. The maximum deviation between the non-corrected and the simulated antenna patterns occurs around -4° where the measured pattern is approximately 15 dB above the simulated −40 dB level. The corrected pattern obtained with the frequency shift method corresponds very well to the simulated pattern. Generally the corrected pattern differs less than 2 dB from the simulated pattern. The only exception occurs at 7° where the side lobe level of the corrected pattern differs 3 dB from the simulated one.

The corrected pattern obtained with APC technique corresponds well with the simulated pattern. The accuracy provided

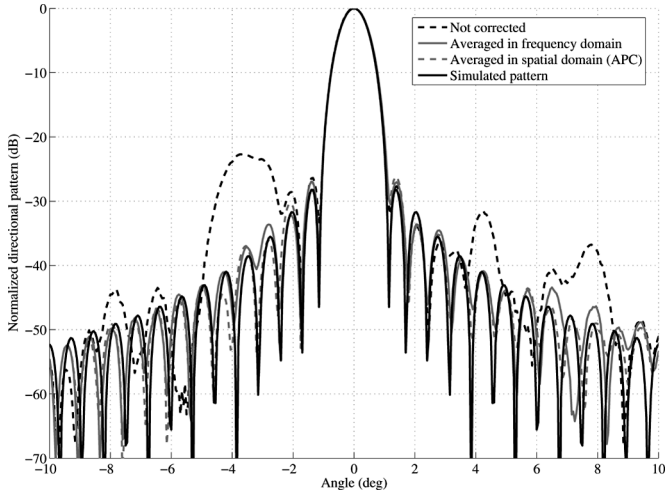

Fig. 7. Antenna patterns of the test antenna. The solid black line is the simulated pattern, the dashed black line is the noncorrected pattern, the solid gray line is the pattern obtained with frequency shift method and the dashed gray line is the pattern obtained with the APC technique.

by the APC technique is approximately equal to the accuracy provided by the frequency shift technique.

The reason for the decreased correction accuracy of the frequency shift method around 7° are most likely multiple reflections between the AUT and the hologram. As the frequency shift interval is 500 MHz, the interference period between the original and shifted signals is 0.6 m. Therefore, if the path length of the signal is a multiple of 0.6 m, the frequency shift of 500 MHz does not change the phase of the signal and the effect of the reflected signal can not be compensated. The distance between the AUT and the hologram is 1.8 m, which is a multiple of 0.6 m. The results with the APC technique support the assumption of multiple reflections. As the AUT is displaced transversally, the distance between the AUT and the hologram is changed due to the 33° offset angle of the hologram and therefore APC technique is able to correct the antenna pattern. In addition, this phenomenon is not seen with the virtual antenna. The multiple reflections between the AUT and the hologram are probably much weaker than those with a large aperture test antenna as the virtual antenna aperture is formed by probing the quiet-zone field with a small probe.

V. Conclusion

Originally developed for low radio frequencies, the frequency shift method has not been seen attractive due to required bandwidth requirements. In this paper, the applicability of the method at millimeter and submillimeter wavelengths is pointed out. The feasibility of the method in a hologram-based CATR is studied analytically and its operation is verified experimentally. Experimental results reveal that the frequency shift technique is able to correct spurious signals originating from the hologram. The correction accuracy in the test case is equal to that of the APC technique. However, the frequency shift technique requires less measurement time and is easier to implement. The method can also be used for range evaluation purposes. The uncertainty analysis for the corrected antenna pattern is a topic of a future research.

ACKNOWLEDGMENT

The authors would like to thank Mr. E. Kahra and Mr. H. Rönnberg for help in manufacturing the test antenna and other fine mechanical parts. They would also like to thank Mr. T. Koskinen and Ms. A. Lönnqvist for their contribution in developing the hologram-based compact antenna test range at TKK.

REFERENCES

[1] T. Hirvonen, J. Ala-Laurinaho, J. Tuovinen, and A. V. Räisänen, "A compact antenna test range based on a hologram," *IEEE Trans. Antennas Propag.*, vol. 45, no. 8, pp. 1270–1276, Aug. 1997.

[2] J. Häkli, T. Koskinen, A. Lönnqvist, J. Säily, J. Mallat, J. Ala-Laurinaho, V. Viikari, A. V. Räisänen, and J. Tuovinen, "Testing of a 1.5 m reflector antenna at 322 GHz in a CATR based on a hologram," *IEEE Trans. Antennas Propag.*, vol. 53, no. 10, pp. 3142–3150, Oct. 2005.

[3] A. Lönnqvist, T. Koskinen, J. Häkli, J. Säily, J. Ala-Laurinaho, J. Mallat, V. Viikari, J. Tuovinen, and A. V. Räisänen, "Hologram-based compact range for submillimeter wave antenna testing," *IEEE Trans. Antennas Propag.*, vol. 53, no. 10, pp. 3151–3159, Oct. 2005.

[4] J. Ala-Laurinaho, T. Hirvonen, P. Piironen, A. Lehto, J. Tuovinen, A. V. Räisänen, and U. Frisk, "Measurement of the Odin telescope at 119 GHz with a hologram-type CATR," *IEEE Trans. Antennas Propag.*, vol. 49, no. 9, pp. 1264–1270, Sep. 2001.

[5] A. M. Predoehl and W. L. Stutzman, "Implementation and results of a time-domain gating system for far-field range," in *Proc. 19th Annu. Meeting Symp. Antenna Measurement Techniques Association (AMTA)*, Oct. 1997, pp. 8–12.

[6] J. Appel-Hansen, "Reflectivity level of radio anechoic chambers," *IEEE Trans. Antennas Propag.*, vol. AP-21, no. 4, pp. 490–498, Apr. 1973.

[7] V. Viikari, J. Häkli, J. Ala-Laurinaho, J. Mallat, and A. V. Räisänen, "A feed scanning based APC technique for compact antenna test ranges," *IEEE Trans. Antennas Propag.*, vol. 53, no. 10, pp. 3160–3165, Oct. 2005.

[8] R. E. Hiatt, E. F. Knott, and T. B. A. Senior, A study of VHF absorbers and anechoic rooms Radiation Lab., Univ. Michigan, Ann Arbor, MI, Tech. Rep. 5391-1-F, 1963.

[9] V. Viikari, J. Mallat, J. Ala-Laurinaho, J. Häkli, and A. V. Räisänen, "Antenna pattern correction in a hologram CATR based on averaging in frequency domain," in *Proc. 27th Annu. Meeting Symp. Antenna Measurement Techniques Association (AMTA)*, Oct. 2005, pp. 341–345.

[10] P. S. Hacker and H. E. Schrank, "Range distance requirements for measuring low and ultralow sidelobe antenna patterns," *IEEE Trans. Antennas Propag.*, vol. AP-30, no. 5, pp. 956–966, Sep. 1982.

Ville Viikari (S'04) was born in Espoo, Finland, in 1979. He received the M.Tech. degree in electrical engineering from the Helsinki University of Technology (TKK), Espoo, Finland, in 2004, and is currently working toward the D.Tech. degree at the same university .

Since 2001, he has been a Trainee, Research Assistant, and Research Engineer with the Radio Laboratory at TKK. His current research interest is the development of the antenna measurement techniques at sub-millimeter wavelengths.

Juha Mallat was born in Lahti, Finland, in 1962. He received the Diploma Engineer (M.Sc.) with honors, and the Lic.Tech. and D.Sc. (Tech.) degrees in electrical engineering from the Helsinki University of Technology (TKK), Espoo, Finland, in 1986, 1988, and 1995, respectively.

He has been with the TKK Radio Laboratory (and its Millimeter Wave Group) since 1985, working as a Research Assistant, Senior Teaching Assistant, and Research Associate until 1994. From 1995 to 1996, he was a Project Manager and Coordinator on an education project between TKK and the Turku Institute of Technology. Since 1997, he has been a Senior Scientist in MilliLab (Millimeter Wave Laboratory of Finland—ESA External Laboratory), with the exception of a period of one year during 2001–2002 when he served as a Professor (*pro tem*) of Radio Engineering at TKK. His research interests and experience cover various topics in radio engineering applications and measurements, especially at millimeter wave frequencies. He has also been involved in building and testing millimeter wave receivers for space applications.

Juha Ala-Laurinaho was born in Parkano, Finland, in 1969. He received the Diploma Engineer (M.Sc.) degree in mathematics, and the Lic.Sc. (Tech.) and D.Sc. (Tech.) degrees in electrical engineering from the Helsinki University of Technology, Espoo, Finland, in 1995, 1998, and 2001, respectively.

Since 1995, he has worked as a Research Assistant, Research Engineer, and Project Manager at the Radio Laboratory of the Helsinki University of Technology. His current research interest is the development of the antenna measurement techniques for millimeter and submillimeter wavelengths.

Janne Häkli (S'97–M'05) was born in Helsinki, Finland, in 1972. He received the Diploma Engineer (M.Sc.) degree in 1999 and Licentiate of Science (Tech.) degree in 2002, both in electrical engineering, from the Helsinki University of Technology (TKK), Espoo, Finland. He is currently working toward the D.Sc. (Tech.) degree.

He has been with the Radio Laboratory of TKK since 1998, working as a Research Assistant and a Research Engineer. His current research interests include submillimeter wave shaped reflector antennas, antenna measurement techniques, and hologram applications.

Antti V. Räisänen (S'76–M'81–SM'85–F'94) received the Doctor of Science (Tech.) degree in electrical engineering from the Helsinki University of Technology (TKK), Espoo, Finland, in 1981.

He was appointed to the Professor Chair of Radio Engineering at TKK in 1989, after holding the same position as an Acting Professor in 1985 and 1987–1989. He has held Visiting Scientist and Professor positions at the Five College Radio Astronomy Observatory (FCRAO), the University of Massachusetts, Amherst (1978–1981), Chalmers University of Technology, Göteborg, Sweden (1983), the Department of Physics, University of California, Berkeley (1984–1985), the Jet Propulsion Laboratory and California Institute of Technology, Pasadena (1992–1993), and the Paris Observatory and the University of Paris 6, Paris, France (2001–2002). He is currently supervising research in millimeter-wave components, antennas, receivers, microwave measurements, etc., at TKK Radio Laboratory and MilliLab (Millimeter Wave Laboratory of Finland–ESA External Laboratory). The Smart and Novel Radios Research Unit (SMARAD), led by Dr. Räisänen at TKK, obtained in 2001 the national status of Center of Excellence in Research from the Academy of Finland after competition and international review. He has authored and coauthored some 400 scientific or technical papers and six books, e.g., *Radio Engineering for Wireless Communication and Sensor Applications* (Norwell, MA: Artech House, 2003). He also coauthored the chapter "Radio-Telescope Receivers" in *Radio Astronomy* (Powell, OH: Cygnus-Quasar Books, 2nd ed., 1986).

Dr. Räisänen was Secretary General of the 12th European Microwave Conference in 1982. He was Chairman of the IEEE MTT/AP Chapter in Finland from 1987 to 1992. He was Conference Chairman for the 22nd European Microwave Conference in 1992 and for the 2nd ESA Workshop on Millimeter Wave Technology and Applications: antennas, circuits and systems in 1998, and Co-Chair for the 3rd ESA Workshop on Millimeter Wave Technology and Applications: Circuits, Systems, and Measurement Techniques in 2003. In 2006, he is Conference Chairman of the International Joint Conference of the 4th ESA Workshop on Millimeter-Wave Technology and Applications, the 8th Topical Symposium on Millimeter Waves TSMMW2006, and the 7th MINT Millimeter-Wave International Symposium MINT-MIS2006. During 1995–97 he served in the Research Council for Natural Sciences and Engineering, the Academy of Finland. From 1997 to 2000, he was Vice-Rector for Research and International Relations of TKK. He served as an Associate Editor of the IEEE TRANSACTIONS ON MICROWAVE THEORY AND TECHNIQUES from 2002 to 2005.